

RISE Video Dataset: Recognizing Industrial Smoke Emissions

Yen-Chia Hsu¹, Ting-Hao (Kenneth) Huang², Ting-Yao Hu¹, Paul Dille¹, Sean Prendi¹, Ryan Hoffman¹, Anastasia Tshlares¹, Randy Sargent¹, Illah Nourbakhsh¹

¹Carnegie Mellon University, Pittsburgh, PA, USA

²Pennsylvania State University, State College, PA, USA

¹{yenchiah, tingyaoh, pdille, sprendi, ryanhoff, anastt, rsargent, illah}@andrew.cmu.edu, ²txh710@psu.edu

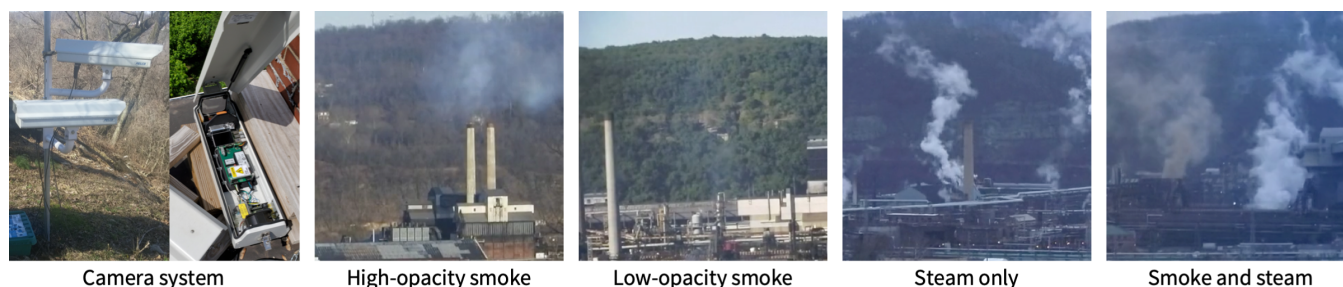


Figure 1: Samples in our dataset and the deployed camera system for monitoring industrial emissions at various sites.

ABSTRACT

Industrial smoke emissions pose a significant concern to human health. Prior works have shown that using Computer Vision (CV) techniques to identify smoke as visual evidence can influence the attitude of regulators and empower citizens in pursuing environmental justice. However, existing datasets do not have sufficient quality nor quantity for training robust CV models to support air quality advocacy. We introduce **RISE, the first large-scale video dataset for Recognizing Industrial Smoke Emissions**. We adopt the citizen science approach to collaborate with local community members in annotating whether a video clip has smoke emissions. Our dataset contains 12,567 clips with 19 distinct views from cameras on three sites that monitored three different industrial facilities. The clips are from 30 days that spans four seasons in two years in the daytime. We run experiments using deep neural networks developed for video action recognition to establish a performance baseline and reveal the challenges for smoke recognition. Our data analysis also shows opportunities for integrating citizen scientists and crowd workers into the application of Artificial Intelligence for social good.

KEYWORDS

Dataset, community citizen science, computer vision, air pollution, smoke recognition, human-computer interaction, sustainability, AI for social good, community empowerment

1 INTRODUCTION

Air pollution has been associated with adverse impacts on human health, including respiratory and cardiovascular diseases [13, 28, 41]. According to the United States Environmental Protection Agency (US EPA), hazardous air pollutants (e.g., smoke) emitted from industrial sources pose a significant concern [4]. Currently, citizens who wish to advocate for better air quality rely on a manual approach developed by the US EPA to determine if smoke emissions

violate the issued permit to the facility [3]. This manual approach involves going into the field and taking multiple measurements, which is time-consuming and laborious. Prior works have shown that using Computer Vision to identify industrial smoke emissions automatically as visual evidence can empower citizens in pursuing environmental justice and influence the attitude of regulators [21, 22]. This type of data-driven evidence, especially when integrated with community narratives, is essential for citizens to make sense of local environmental issues and take community action [21, 39].

However, it is expensive and challenging to collect large-scale images or videos of real-world industrial smoke emissions, which are required to develop a practical smoke recognition model. Recent state-of-the-art models, deep neural networks, are typically data-hungry. Training these networks with insufficient data may lead to overfitting and raise concerns for application, such as high false alarm rates. Table 1 lists all the current datasets for smoke recognition, in which we count the number of videos and frames (using the `ffprobe` command in FFmpeg [1]) based on the data that are publicly available.¹ Compared to datasets for object and action recognition, such as ImageNet [45] and Kinetics [29], existing datasets for smoke recognition are relatively small. Despite several successes in the prior works of using deep learning for smoke detection [5, 15, 24, 33, 38, 55–60, 63], these models were trained and evaluated on relative small video or image datasets (Table 1). In response to data sparsity, some prior works attempted to generate artificial smoke images, where smoke emissions with transparent background were synthesized with various scenes [55, 61, 63]. But such synthetic data can not capture the rich behavior and appearance of smoke under real-world conditions, such as weather.

¹ Some datasets treat steam as smoke, and we count the number of smoke frames within these datasets only based on the videos that do not involve steam. Moreover, some datasets contain videos for fire detection, and we did not count them in this table since fire detection is not our focus in this research.

Table 1: Comparison of publicly available datasets for recognizing smoke. This table does not involve unlabeled or synthetic data. Symbol “...” means not applied, where the corresponding datasets are image-based. The asterisk symbol * means that the dataset provides labels on image patches that do not provide sufficient context for the surroundings. The dagger symbol † means that the dataset uses satellite images, and therefore the sources of smoke emissions are unidentifiable. In the first column, the first reference means the paper, and the second reference shows the public link to the dataset. For the columns that have only one reference, the dataset link is in the referred paper.

	# of scenes	# of labeled clips	# of frames (images)	Average # of frames per clip	Ratio of smoke frames	Has temporal data?	Has context?	Is from industrial sources?	Appearance change level
This Work	19	12,567	452,412	36	41%	yes	yes	yes	high
Bugaric <i>et al.</i> [6]	10	10	213,909	21,391	100%	yes	yes	no	low
Ko <i>et al.</i> [30, 53]	16	16	43,090	1,514	37%	yes	yes	no	low
Dimitropoulos <i>et al.</i> [12, 16]	22	22	17,722	806	56%	yes	yes	no	low
Toreyin <i>et al.</i> [11, 52]	21	21	18,031	820	98%	yes	yes	no	low
Filonenko <i>et al.</i> [15]*	...	396	100,968	255	61%	yes	no	no	low
Xu <i>et al.</i> [57, 62]	5,700	...	49%	no	yes	no	low
Xu <i>et al.</i> [55, 62]	3,578	...	100%	no	yes	no	low
Xu <i>et al.</i> [56, 62]	10,000	...	50%	no	yes	no	low
Ba <i>et al.</i> [5]*†	6,225	...	16%	no	no	unknown	medium
Lin <i>et al.</i> [34, 62]*	16,647	...	29%	no	no	no	low
Yuan <i>et al.</i> [14, 60]*	24,217	...	24%	no	no	no	low

In addition to the challenge of data scarcity, most existing smoke recognition datasets do not have sufficient quality for training deep learning models. Most of them are from burning materials (*e.g.*, in laboratories) and fire events (*e.g.*, wildfire) at specific times, which have low temporal appearance changes. Moreover, none of the existing datasets contain smoke emissions from industrial sources (*e.g.*, stack emissions and fugitive emissions). About a third of the datasets in Table 1 are imbalanced (ratio of smoke frames higher than 80% or less than 20%). Also, the average number of frames per labeled clip is high in these datasets, which shows weak temporal localization.

This paper introduces RISE, the first large-scale video dataset for recognizing industrial smoke emissions. We built and deployed a camera network on various sites since early 2017 to monitor industrial activities of petroleum coke plants (Figure 1, left). We collaborated with air quality grassroots communities in installing the cameras, which capture an image approximately every 10 seconds. These images were streamed back to our servers for stitching into panoramas and stacking into timelapse videos. From these panorama timelapse videos, we cropped clips based on domain knowledge about where the smoke emissions frequently occur. Finally, these clips were labeled by citizen scientists (volunteers) to indicate whether smoke emissions are present by using a web-based video labeling system that we developed (Figure 2 and 3).

RISE consists of clips from 30 different days in the daytime (6 am to 8 pm), which span four seasons in two years. Also, the labeled video clips contain 19 different views cropped from three panoramas taken by cameras at three distinct locations. The dataset covers various characteristics of smoke emissions, including opacity and color, under diverse weather (*e.g.*, haze, fog, snow, cloud) and lighting conditions. Moreover, the dataset involves distractions of various types of steam, which can be similar to smoke and can be challenging to distinguish. Figure 1 shows sample clips. We used the dataset to train an Inflated 3D Convolutional Neural Network (I3D ConvNet) [9] as a baseline benchmark. We also applied Grad-CAM to visualize activated regions, which help us diagnose if the network

can focus on areas that have smoke emissions. Also, we compare the labeling quality among citizen scientists and Amazon Mechanical Turkers (MTurkers). The code and the RISE dataset for training the network² are all open-sourced and available for public access, same for the video labeling system³.

2 RELATED WORK

We have discussed the existing datasets for smoke recognition. This section provides an overview of existing smoke recognition techniques and citizen science.

A set of prior works relied on motions, colors, physical-based models, or hand-crafted features for smoke recognition. For instance, Kopilovic *et al.* computed the entropy of the optical flow field to identify smoke [31]. Celik *et al.* used color models to identify smoke pixels [10]. Toreyin *et al.* combined background subtraction, edge flickering, and texture analysis into a final result [52]. Lee *et al.* used change detection to extract candidate regions, computed feature vectors based on color modeling and texture analysis, and trained a support vector machine classifier using these features [32]. Tian *et al.* presents a physical-based model and use sparse coding to extract reliable features for single image smoke detection [51]. Gubbi *et al.* and Calderara *et al.* applied texture descriptors, such as a wavelet transform, on small blocks in an image for obtaining feature vectors and train a classifier using these features [8, 17].

Another set of prior works developed or enhanced various deep learning architectures for smoke recognition. For example, Yuan *et al.* trained two encoder-decoder networks to focus on global contexts and fine details, respectively, for smoke region segmentation [61]. Hu and Lu trained spatial-temporal ConvNets (similar to the two-stream model in action recognition [49]) and applied multi-task learning to avoid computing optical flow for real-time detection [24]. Liu *et al.* fused ResNet (trained with the original RGB images) and ConvNet

²<https://github.com/CMU-CREATE-Lab/deep-smoke-machine>

³<https://github.com/CMU-CREATE-Lab/video-labeling-tool>

Table 2: The number and ratio of video clips for all 19 camera views filtered by various temporal conditions.

	# of labeled clips	Ratio
Has smoke	5,090	41%
In winter (Dec to Feb)	7,292	58%
In spring (Mar to May)	1,057	8%
In summer (Jun to Aug)	2,999	24%
In fall (Sep to Nov)	1,219	10%
From 6 am to 10 am	4,001	32%
From 11 am to 3 pm	6,071	48%
From 4 pm to 8 am	2,495	20%

Table 3: Ratio of the number of videos for each split (rounded to the nearest second digit). Split S_0, S_1, S_2, S_4, S_5 is based on scenes. Split S_3 is based on time sequence.

	S_0	S_1	S_2	S_3	S_4	S_5
Training	.62	.62	.62	.61	.62	.62
Validation	.13	.12	.12	.14	.11	.13
Testing	.25	.26	.26	.25	.26	.25

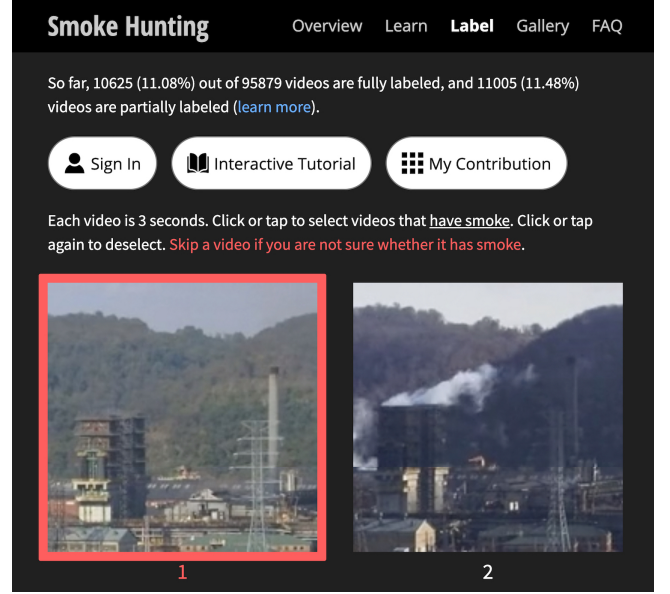
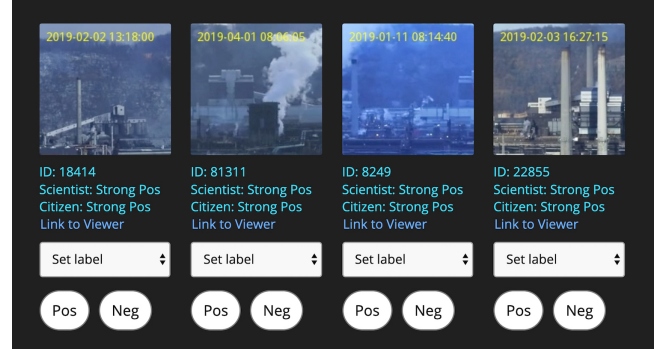
(trained with Dark Channel images [18]) for classifying smoke [38]. There are also works that applied or enhanced object detectors (e.g., SSD [37], MS-CNN [7], Faster R-CNN [44], YOLO [43]) for identifying the regions that have smoke [33, 55, 58, 63]. All these models were trained and evaluated on relatively small datasets (Table 1).

To collect a large dataset for smoke recognition, we adopt citizen science to empower laypeople and experts to produce knowledge jointly [48]. Citizen science has been successfully applied in science-oriented projects, especially when research is so large-scale that it is infeasible for experts to tackle alone. For instance, the PI@ntNet project invites volunteers to submit plant images using mobile applications, and these data are used to develop Computer Vision models to identify plant species automatically [2, 27]. In the case mentioned above, experts define the main research question and invite citizens to participate. In our case, we utilize Computer Vision and data-driven evidence to address concerns that are directly raised by local communities. Specifically, we apply a civic-oriented framework, Community Citizen Science [23], to empower citizens, who are affected by industrial pollution to advocate for better air quality.

3 RISE DATASET

This paper introduces RISE, the first large-scale video dataset for recognizing industrial smoke emissions. RISE dataset consists of 12,567 labeled clips from industrial sources, including those emitted from stacks (i.e., stack emission) and escaped from facilities (i.e., fugitive emission). Each clip has 36 frames (with resolution 180 by 180 pixels), which represent about 6 minutes in real-world time. These clips contain 19 distinct views (Figure 5), where 15 views are cropped from the panorama timelapse at one site, and 4 views are from two other sites. These clips span 30 days across four seasons in two years, from 6 am to 8 pm. Table 2 summarizes the distribution of this dataset across time.

This dataset has six splits (S_0 to S_5 in Table 3), and each split has three different training, validation, and testing sets. Most of the

**Figure 2: A part of the user interface of the smoke labeling system. Users can scroll the page and click (or tap) on the 16 video clips to indicate the presence of smoke emissions.****Figure 3: A part of the user interface of the smoke labeling system for researcher-citizen collaboration. Researchers can quickly confirm the labels provided by volunteers.**

splits (except S_3) are based on scenes, where different views are used for each phase. For these splits, 15 views from one site are spread among all three sets, and four views from two other sites are always in the testing set. In this way, we can estimate the generalizability of models trained with this dataset. Split S_3 is based on time sequence, where the farthestmost 18 days are used for training, the middle 2 days are used for validation, and the nearest 10 days are used for testing. Thus, we can evaluate if models trained with data in the past can be used in the future.

3.1 System for Data Collection

We have built and deployed cameras to monitor pollution sources (Figure 1, left). The physical system uses a Raspberry Pi single-board computer to control a Nikon 1 J5 digital camera. It also has

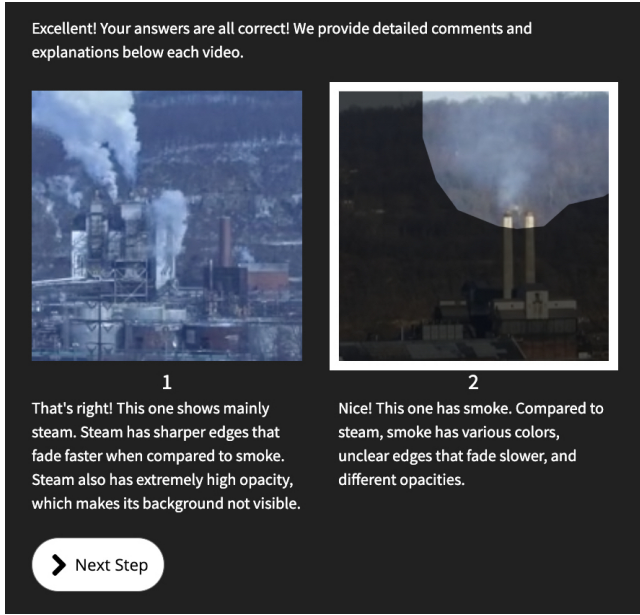


Figure 4: A part of the interactive tutorial for providing step-by-step guidance of labeling smoke emissions.

other features such as a heater and cooler to regulate internal temperatures and a servo motor to enable remote power cycling. The cost per camera is about \$2,000 US dollars. The camera takes a photo approximately every 10 seconds, and the photos are then streamed back to a data processing server for stitching and stacking into panorama timelapse videos.

Deploying the camera system relies heavily on citizen engagement. To build relationships and mutual trusts between our organization and the community, we canvassed the local region, met with affected residents in person, and attended local events (*e.g.*, community meetings and public hearings) to explain our mission. For those residents who are willing to host cameras, our team installs the equipment and offers complimentary Internet services.

3.2 System for Data Annotation

We apply citizen science [26, 48] to invite volunteers to participate in this research and develop a web-based smoke labeling tool to allow volunteers to annotate data. Citizen science opens opportunities to collaborate with residents and advocacy groups, who have diverse expertise in local concerns. Through two workshops with air quality advocates, three presentations in local community events, and two guest lectures in universities, we recruited volunteers to help label smoke emissions using this labeling tool. The design and use of this tool were iteratively refined based on the valuable insights from these community members. For instance, we observed that volunteers enjoy labeling data on tablets. Thus we make sure that the tool works on most modern browsers (*i.e.*, Chrome, Firefox, Safari, Edge) for recent operation systems, including Android, iOS, Windows, and Mac OS. Also, we found that the labeling task can be challenging for volunteers who are not familiar with visual opacity reading [3]. Thus,

we implemented an interactive tutorial to introduce the task with step-by-step guidance (Figure 4). Users are first presented with simplified tasks that explain small concepts, such as the characteristics of smoke and the differences between smoke and steam. After performing each small task, the system shows the answers, explanations, and the regions on the clips that have smoke emissions.

There are two modes of user interfaces for data labeling. The first one (the individual mode) asks volunteers or researchers to label 16 video clips at once (Figure 2). Users can scroll the interface and click (or tap) on the video clips to indicate the presence of smoke emissions. The second one (the collaborative mode) asks researchers to confirm the labels contributed by volunteers. In the collaborative mode, the system shows the answers provided by citizens as prior information, and the researcher can choose to agree with or override these answers. This mode is designed to reduce the mental load for the labeling task and increase the speed of gathering labels at the early stage of system deployment when the amount of users is small.

When labeling, we refer to the 16 clips provided by the system as a page. For quality control, we randomly insert four gold standards (labeled by the researcher), and the system will accept a page and record its labels if the volunteer answers all the gold standards correctly. Otherwise, the page will be discarded. We make sure that at least one negative and positive samples are included in the gold standards to prevent uniform guessing. Besides, each clip is reviewed by at least two different volunteers (identified using Google Analytics tracker). If their answers do not agree with each other, a third volunteer is asked to review the clip. The system takes the majority vote of the answers as the final label for the clip. For information security, we encoded the pages and their labels into JSON Web Tokens with digital signatures issued by the back-end server. Combining with the https protocol, we make sure that the labels sent from the front-end are authentic and valid.

3.3 Analysis of User Contribution

The stable version of the labeling tool was launched in early February 2019. Up to February 24 in 2020 (12 months), the tool has collected 12,567 fully-labeled and 11,402 partially-labeled clips. The partially labeled clips were reviewed by only one volunteer or two volunteers with disagreement, and we did not include them in the dataset due to uncertain data quality. Among the fully-labeled video clips, 42% (5,230) and 20% (2,560) of them are labeled individually by researchers and citizens, respectively, and 38% (4,777) of them are labeled collaboratively.

During the launch period of nine months, we attract 60 volunteers who contributed at least one page that passed the system's quality check. We divide the volunteers into four groups based on their reliability (the acceptance rate of pages) and contributions. For instance, volunteers in the top enthusiast group have higher reliability (greater than or equal to 0.5) and a higher number of accepted pages (greater than or equal to the average of all participants). The analysis of user groups shows that 12% of them contributed 86% of the data, which shows a highly skewed pattern of contribution (Table 4). This group of active users also have high reliability (mean=.76, std=.10), which is the acceptance rate of the labeling pages. This skewed pattern is typical among citizen science projects, where many volunteers participate for only a few times [46].



Figure 5: All views of video clips in the RISE dataset. The rightmost four views are from different sites pointing at another facility.

Table 4: Analysis of the volunteers who contributed at least one page that passes the quality check and accepted by the system. The results are based on 392 positive labels with smoke (54.4% out of total $N=720$ videos). Filtered MTurker is the one with reliability larger than 0.3. The reported format is “mean \pm standard deviation”. Reliability means the acceptance rate of pages (with 16 clips).

User group	# of users	Reliability \forall group	Reliability \forall user	# of accepted pages \forall group	# of accepted pages \forall user
Top Enthusiasts	7 (12%)	.86	.76 \pm .10	1,491 (86%)	213 \pm 328
Other Enthusiasts
Top Volunteers	41 (68%)	.69	.74 \pm .19	218 (13%)	5 \pm 5
Other Volunteers	12 (20%)	.26	.28 \pm .08	18 (1%)	2 \pm 1
All	60 (100%)	.81	.65 \pm .25	1,727 (100%)	29 \pm 125

Table 5: The data quality (simulated 100 times) of citizens and MTurkers, using researcher labels as the ground truth. The results are based on 392 positive labels with smoke (54.4% out of total $N=720$ videos). Filtered MTurker is the one with reliability larger than 0.3. The reported format is “mean \pm standard deviation.”

User group	Precision	Recall	F-score
Citizen	.98	.83	.90
Filtered MTurker	.94 \pm .01	.89 \pm .01	.91 \pm .01
All MTurker	.93 \pm .01	.83 \pm .01	.88 \pm .01

Table 6: The inter-rater agreement (simulated 100 times) of the labels between pairs of MTurker, citizen, and researcher groups. The reported format is “mean \pm standard deviation.”

	Cohen’s kappa
Researcher v.s. Citizen	.80
Researcher v.s. Filtered MTurker	.81 \pm .01
Researcher v.s. All MTurker	.75 \pm .02
Citizen v.s. All MTurker	.72 \pm .02
Citizen v.s. Filtered MTurker	.75 \pm .01

3.4 Analysis and Comparison of Data Quality

We compare the labels produced by three groups: citizens (volunteers), researchers, and crowd workers (MTurkers). To obtain labels from MTurkers, we first randomly sampled 720 clips that were fully-labeled by citizens and researchers from the RISE dataset. We then divided these clips into 60 labeling tasks and added four randomly-sampled gold standards to each task for quality control. The user interface is identical to the one used for citizens. When labeling, we ensured that the MTurkers took the interactive tutorial before

performing the task. We first posted the tutorial task with 50 assignments to Amazon Mechanical Turk (MTurk) (\$1.5 per task) and granted qualifications to the workers who finished the tutorial. We then posted the 60 labeling tasks to MTurk, where each task collects five assignments from different MTurkers. Only the workers who have the qualification can perform our tasks. The estimated time to complete one task is 90 seconds. We paid \$0.25 per task, yielding an estimated hourly wage of \$15. As a result, 14 MTurkers were recruited and accomplished all the tasks in about 12 hours.

The data quality is similar between citizens and filtered MTurkers. The filtered MTurkers is a subset with reliability (*i.e.*, the acceptance rate of the labeling pages) better than 0.3 (random guessing is 0.07). To match the quality-control mechanism used in the deployed labeling tool, we randomly selected 3 assignments for majority voting and simulated for 100 times. Using researcher labels as the ground truth, Table 5 indicates similar strong performance in precision, recall, and f1-score of the positive labels (with smoke). Also, the strong Cohen’s kappa in Table 6 shows a high inter-rater agreement.

4 EXPERIMENTS

We establish a baseline benchmark for RISE dataset by exploiting Inflated 3D Convolutional Neural Network (I3D ConvNet) with Inception-v1 layers [9]. I3D is a representative model for video action recognition based on the inflation of 2D ConvNet. The inputs of this baseline model are RGB frames. The parameters of this model are pretrained on ImageNet [45] and Kinetics [29] datasets, and then finetuned on the training set of RISE. During training, we apply data augmentation techniques, including horizontal flipping, random resizing and cropping, perspective transformation, area erasing, and color jittering. We refer to this baseline model as RGB-I3D. The validation set is used for hyper-parameter tuning.

Table 7: F-scores for comparing the effect of data augmentation on the testing set for each split. Abbreviation ND means no data augmentation.

Model	S_0	S_1	S_2	S_3	S_4	S_5	Average
RGB-I3D	.80	.84	.82	.87	.82	.75	.817
RGB-I3D-ND	.76	.79	.81	.86	.76	.68	.777
RGB-SVM	.57	.70	.67	.67	.57	.53	.618

Table 8: F-scores for comparing the effect of using temporal information on the testing set for each split. Abbreviation FP means with frame perturbation.

Model	S_0	S_1	S_2	S_3	S_4	S_5	Average
RGB-I3D	.80	.84	.82	.87	.82	.75	.817
RGB-I3D-FP	.76	.81	.82	.87	.81	.71	.797
Flow-I3D	.55	.58	.51	.68	.65	.50	.578
Flow-SVM	.42	.59	.47	.63	.52	.47	.517

4.1 Implementation

The parameters of our baseline models are optimized using binary cross-entropy loss and Stochastic Gradient Descent (SGD) with momentum 0.9 for 2,000 steps. Table 10 shows the detail setup of training hyper-parameters. For each step, we perform gradient descent to update the parameters after accumulating the gradients for several iterations (using backward propagation) with a specific batch size. We apply weight decay (regularization) when training the model to prevent overfitting. The initial learning rate starts from a fixed value and decreases by a factor of 0.1 based on predefined milestones. All of the models and training scripts are implemented in PyTorch framework [40], and executed on one machine with four NVIDIA GTX 1080 Ti GPUs. Batch sizes are evenly distributed among all GPUs. When comparing performance among different models, we select the one with the best F-score after 500 training steps. For models that have the same F-score, we select the one with the lowest validation error.

4.2 Result

In order to understand the effectiveness of our baseline, we also train five other models for comparison.

- RGB-I3D-ND is the same baseline model without any data augmentation.
- RGB-SVM exploits Support Vector Machine (SVM) as the classifier, which takes the pretrained I3D features (without finetuning on our dataset) as input.
- RGB-I3D-FP is trained using video clips with frame-wise random permutation.
- Flow-I3D has the same network architecture as our baseline, but processes precomputed TVL1 optical flow frames. It also conducts the same data augmentation pipeline except color jittering.
- Flow-SVM, similar to RGB-SVM, uses raw I3D features extracted with optical flow frames.

The implementation details of these I3D models are the same as the aforementioned. For the deep neural network models that are not mentioned in Table 10, they use the same hyper-parameters as the RGB-I3D model. From the experiment results, we can make the

following observations. First, results in Table 7 show that the I3D model outperforms SVM by a large margin, and data augmentation can further improve the performance. Second, from results in Table 8, we can see that frame-wise permutation does not degrade the performance much, and Flow-based models perform worse than their RGB counterparts. This observation indicates the challenge of using temporal information within this dataset. To further understand this challenge, we train the other five variations based on RGB-I3D with different temporal processing techniques.

- RGB-I3D-NL wraps two Non-Local (NL) blocks [54] in the last Inception layer (closest to the output) around the 3D convolution blocks with kernel size larger than one. NL blocks are designed to capture long-range dependencies by modeling interactions among features in both space and time.
- RGB-I3D-LSTM attaches one Long Short-Term Memory (LSTM) layer [19] with 128 hidden units after the last Inception layer. LSTM is a type of recurrent neural network with a gating mechanism to regulate the flow of temporal information. We finetune this LSTM variation from the best RGB-I3D model with the I3D layers frozen.
- RGB-I3D-TSM wraps Temporal Shift modules (TSM) [35] around each Inception layer. This TSM variation shifts 1/4 of the channels along the temporal dimension. This shifting technique is proposed to facilitate exchanging information among nearby video frames.
- RGB-I3D-TC attaches one Timeception (TC) layer [25] after the last Inception layer, using 1.25 as the channel expansion factor. This variation is our best baseline model (Table 11). TC is designed to learn long-range dependencies with simplified and multi-scale kernels, where each convolution kernel has a different scale and is operated on only one temporal dimension. We finetune this TC variation from the best RGB-I3D model with the I3D layers frozen, as used in the original paper.

Results in Table 9 indicate that these techniques do not outperform the baseline model significantly, which confirms the challenge of using the temporal information.

4.3 Visualization

To verify the semantic concept captured by our baseline model, we apply the Gradient-weighted Class Activation Mapping (Grad-CAM [47]) for visualization. This technique analyzes the gradient signal that flowed into the last convolutional layer and generates a localization heatmap, which highlights the important areas for prediction. Ideally, our model should focus on the regions identifying smoke emissions, instead of other objects in the background (e.g., stacks, plant facilities). Therefore, we show true positive cases for fugitive emissions (Figure 6), stack emissions (Figure 8), and co-existence of both smoke and steam (Figure 7). Also, we show a false positive case when steam looks like smoke (Figure 9), another false positive case that cloud shadow is misclassified as smoke (Figure 10), and a negative case where the smoke emission has a small amount for a short duration (Figure 11). These figures show the time sequence from left to right, sampled from 36 frames for every 9 frames.

Table 9: F-scores for comparing different types of temporal models. Abbreviation NL means the Non-Local module [54]. Abbreviation TSM indicates the Temporal Shift module [35]. Abbreviation TC and LSTM means adding the Timeception layers [25] and the Long Short-Term Memory layers [19], respectively.

Model	S_0	S_1	S_2	S_3	S_4	S_5	Average
RGB-I3D	.80	.84	.82	.87	.82	.75	.817
RGB-I3D-TSM	.81	.84	.82	.87	.80	.74	.813
RGB-I3D-LSTM	.80	.84	.82	.85	.83	.74	.813
RGB-I3D-NL	.81	.84	.83	.87	.81	.74	.817
RGB-I3D-TC	.81	.84	.84	.87	.81	.77	.823

Table 10: Hyper-parameters for training models. Symbol η and i indicate the initial learning rate and gradient accumulation iterations, respectively. Milestones are the global steps to decrease the learning rate by a factor of 0.1.

Model	η	Weight decay	i	Batch size	Milestones
RGB-I3D	0.1	10^{-6}	2	40	(500, 1500)
RGB-I3D-TSM	0.1	10^{-10}	1	40	(1000, 2000)
RGB-I3D-LSTM	0.1	10^{-4}	1	32	(1000, 2000)
RGB-I3D-NL	0.1	10^{-6}	2	40	(500, 1500)
RGB-I3D-TC	0.1	10^{-6}	1	32	(1000, 2000)

Table 11: Evaluation of the best baseline model (RGB-I3D-TC) on the testing set for each split. ROC/AUC means area under the receiver operating characteristic curve.

Metric	S_0	S_1	S_2	S_3	S_4	S_5	Average
Precision	.87	.84	.92	.88	.88	.78	.862
Recall	.76	.83	.77	.87	.76	.76	.792
F-score	.81	.84	.84	.87	.81	.77	.823
ROC/AUC	.90	.94	.94	.95	.92	.91	.927

5 DISCUSSION

Exploiting Temporal Information. The experiment results show that the temporal information in our dataset is challenging to utilize. The visualization also shows that the model has limitation in excluding steam (Figure 9), omitting fast-moving cloud shadow (Figure 10), and identifying small-amount smoke emissions (Figure 11). This limitation may come from the difficulty of finding clear correspondence points across frames because smoke emissions, unlike objects, have dynamic and ambiguous shapes. Moreover, our data have a low temporal resolution (10 seconds in real-world time per frame), which means that the pixel displacements are large and can exacerbate this difficulty. Developing methods to efficiently use the temporal information in timelapse videos for smoke-like particles remains an open research question.

Lesson Learned from the Citizen Science Approach. When collecting the RISE dataset with the citizen science approach, we encountered challenges that may offer implications when developing AI systems for social good. First, setting up cameras to collect air pollution dataset requires substantial community outreach efforts since people who were severely affected by air pollution tend to

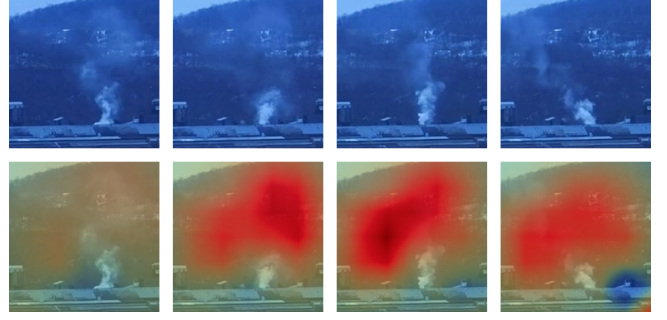


Figure 6: True positive of fugitive emissions in the testing set from split S_0 . The time sequence starts from the left to the right.



Figure 7: True positive of the view that has both smoke and steam emissions in the testing set from split S_0 .

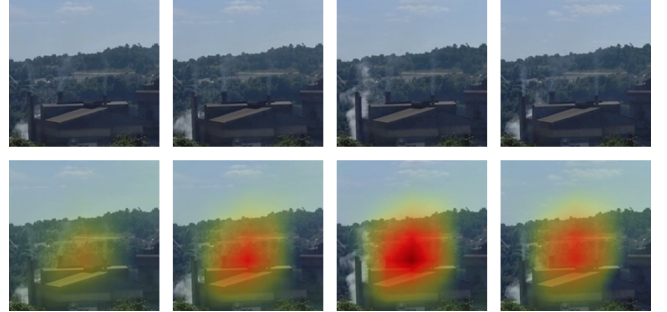


Figure 8: True positive of stack emissions in the testing set from split S_1 . This view is from the site that is not used for training or validation.

be financially impoverished. To them, improving local air quality may not be their top priority. Second, industrial smoke emissions, unlike general object recognition, are not intuitive to identify. From the two workshops that we collaborated with air quality advocacy groups in labeling smoke, we found that the task requires training to understand the color, opacity, and motion of smoke. Third, air pollution issues, unlike other citizen science projects in astronomy (e.g., Galaxy Zoo [36]) or bird watching (e.g., eBird [50]), may not be enjoyable. This characteristic makes it hard to push out this smoke labeling project to the general public. One possible direction is to recruit MTurkers for collecting labels. However, citizen science has been proven useful in empowering residents to address air pollution [20, 21]. Inviting community members to label data



Figure 9: False positive of steam (in the testing set from split S_0) that looks similar to smoke.

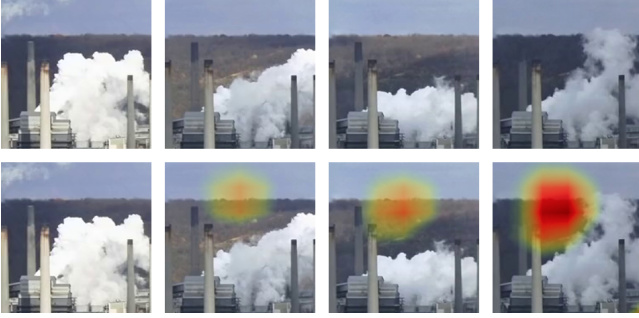


Figure 10: False positive of fast-moving cloud shadow (in the testing set from split S_0) that is misclassified as smoke.



Figure 11: False negative of smoke (in the testing set from split S_0) that emits in a small amount within a short duration.

may increase their awareness and the confidence of tackling local concerns. We leave this research direction to future work.

Integrating Citizen Science and Crowdsourcing. The analysis of data quality demonstrates similar performance between citizen scientists and MTurkers. This result suggests new opportunities for integrating citizen science and crowdsourcing due to their resembling data quality. For instance, at the early stage of system development, if there is a need to develop a model that can generate visual evidence to motivate volunteers, one can recruit MTurkers to label an initial small-scale dataset. Once the model is trained with the initial dataset, one can use it to produce evidence that can attract active citizen scientists who are willing to contribute data. At this stage, the model accuracy may not reach the desired level, and human intervention

may need to be involved. However, as the community’s attention starts to increase, it would be possible to collect more labels and improve model performance over time. A future direction is to ask expert citizens who received the training of visual opacity reading [3] to provide finer labels, such as the opacity and shape of smoke.

Limitations. This work has several limitations. First, in the data quality analysis, it may be unfair to compare the reliability between citizens and MTurkers directly. Due to the difference in their label aggregation logic, it is impossible to know the exact number of volunteers who completed the selected 720 video clips in the analysis. Second, our dataset does not include nighttime video clips, which are difficult for human eyes to identify due to insufficient light. Third, this dataset currently does not offer bounding box labels. We applied domain knowledge to predetermine the locations that smoke emissions were likely to occur, which makes smoke recognition a classification instead of a detection problem. Finally, there exist other ways for aggregating labels provided by researchers and citizens, such as EM-based methods [42]. In our case, researchers always override the decisions made by citizens. We leave the expansion of the different label types and also the methodology for aggregation decisions from different user groups to future work.

6 CONCLUSION

We have described a new large video dataset for recognizing industrial smoke emissions. By collaborating with citizen scientists, we have annotated 12,567 clips that contain 19 views and span 30 days across seasons in two years. The abundant temporal appearance changes of smoke emissions and other distractions (e.g., steam) under various weather conditions open research opportunities for using Computer Vision in addressing air pollution issues. Using this dataset, we have trained an Inflated 3D Convolutional Neural Network as the baseline model for comparison. We have found that it is challenging to use the temporal information in this dataset efficiently. By randomly choosing a subset for comparing data quality, we have found that citizen scientists and Amazon Mechanical Turkers have similar reliability. These findings suggest possible future directions in model improvements and new collaboration methods between citizen science and crowdsourcing.

ACKNOWLEDGMENTS

We thank GASP (Group Against Smog and Pollution), Clean Air Council, ACCAN (Allegheny County Clean Air Now), Breathe Project, NVIDIA, and the Heinz Endowments for the support of this research. We also greatly appreciate the help of our volunteers, which includes labeling videos and providing feedback in system development.

REFERENCES

- [1] n.d.. FFmpeg. <https://www.ffmpeg.org>. (n.d.).
- [2] n.d.. Pl@ntNet. <https://plantnet.org/en/>. (n.d.).
- [3] United States Environmental Protection Agency. n.d.. Method 9 - Visual Opacity. <https://www.epa.gov/emc/method-9-visual-opacity>. (n.d.).
- [4] United States Environmental Protection Agency. n.d.. Stationary Sources of Air Pollution <https://www.epa.gov/stationary-sources-air-pollution>. (n.d.).
- [5] Rui Ba, Chen Chen, Jing Yuan, Weiguo Song, and Siuming Lo. 2019. SmokeNet: Satellite Smoke Scene Detection Using Convolutional Neural Network with Spatial and Channel-Wise Attention. *Remote Sensing* 11, 14 (2019), 1702.

- [6] Marin Bugarić, Toni Jakovčević, and Darko Stipaničev. 2014. Adaptive estimation of visual smoke detection parameters based on spatial data and fire risk index. *Computer vision and image understanding* 118 (2014), 184–196.
- [7] Zhaowei Cai, Quanfu Fan, Rogerio S Feris, and Nuno Vasconcelos. 2016. A unified multi-scale deep convolutional neural network for fast object detection. In *European conference on computer vision*. Springer, 354–370.
- [8] Simone Calderara, Paolo Piccinini, and Rita Cucchiara. 2008. Smoke Detection in Video Surveillance: A MoG Model in the Wavelet Domain. In *Computer Vision Systems*. Lecture Notes in Computer Science, Vol. 5008. Springer Berlin Heidelberg, 119–128.
- [9] Joao Carreira and Andrew Zisserman. 2017. Quo vadis, action recognition? a new model and the kinetics dataset. In *proceedings of the IEEE Conference on Computer Vision and Pattern Recognition*. 6299–6308.
- [10] Turgay Çelik, Hüseyin Özkaramanli, and Hasan Demirel. 2007. Fire and smoke detection without sensors: Image processing based approach. In *European Signal Processing Conference*. 1794–1798.
- [11] Enis Cetin. n.d.. Computer vision based fire detection software. <http://signal.ee.bilkent.edu.tr/VisiFire/Demo/SmokeClips/>. (n.d.).
- [12] Kosmas Dimitropoulos, Panagiotis Barmoutis, and Nikos Grammalidis. 2014. Spatio-temporal flame modeling and dynamic texture analysis for automatic video-based fire detection. *IEEE transactions on circuits and systems for video technology* 25, 2 (2014), 339–351.
- [13] Douglas W. Dockery, C. Arden Pope, Xiping Xu, John D. Spengler, James H. Ware, Martha E. Fay, Benjamin G. Jr. Ferris, and Frank E. Speizer. 1993. An Association between Air Pollution and Mortality in Six U.S. Cities. *New England Journal of Medicine* 329, 24 (1993), 1753–1759. <https://doi.org/10.1056/NEJM199312093292401> PMID: 8179653.
- [14] University of Science Feiniu Yuan, State Key Lab of Fire Science and Technology of China. n.d.. Video Smoke Detection. <http://staff.ustc.edu.cn/~yfn/vsd.html>. (n.d.).
- [15] Alexander Filonenko, Laksono Kurniangggoro, and Kang-Hyun Jo. 2017. Smoke Detection on Video Sequences Using Convolutional and Recurrent Neural Networks. In *International Conference on Computational Collective Intelligence*. Springer, 558–566.
- [16] Nikos Grammalidis, Kosmas Dimitropoulos, and Enis Cetin. n.d.. FIRESENSE database of videos for flame and smoke detection. <https://doi.org/10.5281/zenodo.836749>. (n.d.).
- [17] Jayavardhana Gubbi, Slaven Marusic, and Marimuthu Palaniswami. 2009. Smoke detection in video using wavelets and support vector machines. *Fire Safety Journal* 44 (2009), 1110 – 1115.
- [18] Kaiming He, Jian Sun, and Xiaoou Tang. 2010. Single image haze removal using dark channel prior. *IEEE transactions on pattern analysis and machine intelligence* 33, 12 (2010), 2341–2353.
- [19] Sepp Hochreiter and Jürgen Schmidhuber. 1997. Long short-term memory. *Neural computation* 9, 8 (1997), 1735–1780.
- [20] Yen-Chia Hsu, Jennifer Cross, Paul Dille, Michael Tasota, Beatrice Dias, Randy Sargent, Ting-Hao (Kenneth) Huang, and Illah Nourbakhsh. 2019. Smell Pittsburgh: Community-empowered Mobile Smell Reporting System. In *Proceedings of the 24th International Conference on Intelligent User Interfaces (IUI '19)*. ACM, New York, NY, USA, 65–79. <https://doi.org/10.1145/3301275.3302293>
- [21] Yen-Chia Hsu, Paul Dille, Jennifer Cross, Beatrice Dias, Randy Sargent, and Illah Nourbakhsh. 2017. Community-Empowered Air Quality Monitoring System. In *Proceedings of the 2017 CHI Conference on Human Factors in Computing Systems (CHI '17)*. ACM, New York, NY, USA, 1607–1619. <https://doi.org/10.1145/3025453.3025853>
- [22] Yen-Chia Hsu, Paul S. Dille, Randy Sargent, and Illah Nourbakhsh. 2016. *Industrial Smoke Detection and Visualization*. Technical Report CMU-RI-TR-16-55. Carnegie Mellon University, Pittsburgh, PA.
- [23] Yen-Chia Hsu and Illah Nourbakhsh. 2020. When human-computer interaction meets community citizen science. *Commun. ACM* 63, 2 (2020), 31–34.
- [24] Yaocong Hu and Xiaobo Lu. 2018. Real-time video fire smoke detection by utilizing spatial-temporal ConvNet features. *Multimedia Tools and Applications* 77, 22 (2018), 29283–29301.
- [25] Noureddien Hussein, Efstratios Gavves, and Arnold WM Smeulders. 2019. Timeception for complex action recognition. In *Proceedings of the IEEE Conference on Computer Vision and Pattern Recognition*. 254–263.
- [26] Alan Irwin. 2002. *Citizen science: A study of people, expertise and sustainable development*. Routledge.
- [27] Alexis Joly, Hervé Goëau, Julien Champ, Samuel Dufour-Kowalski, Henning Müller, and Pierre Bonnet. 2016. Crowdsourcing biodiversity monitoring: how sharing your photo stream can sustain our planet. In *Proceedings of the 24th ACM international conference on Multimedia*. 958–967.
- [28] Marilena Kampa and Elias Castanas. 2008. Human health effects of air pollution. *Environmental Pollution* 151, 2 (2008), 362 – 367. Proceedings of the 4th International Workshop on Biomonitoring of Atmospheric Pollution (With Emphasis on Trace Elements).
- [29] Will Kay, Joao Carreira, Karen Simonyan, Brian Zhang, Chloe Hillier, Sudheendra Vijayanarasimhan, Fabio Viola, Tim Green, Trevor Back, Paul Natsev, et al. 2017. The kinetics human action video dataset. *arXiv preprint arXiv:1705.06950* (2017).
- [30] ByoungChul Ko, JunOh Park, and Jae-Yeal Nam. 2013. Spatiotemporal bag-of-features for early wildfire smoke detection. *Image and Vision Computing* 31, 10 (2013), 786–795.
- [31] I. Kopilovic, B. Vagvolgyi, and T. Sziranyi. 2000. Application of panoramic annular lens for motion analysis tasks: surveillance and smoke detection. In *Pattern Recognition, 2000. Proceedings. 15th International Conference on*, Vol. 4. 714–717 vol.4.
- [32] Chen-Yu Lee, Chin-Teng Lin, Chao-Ting Hong, Miin-Tsair Su, et al. 2012. Smoke detection using spatial and temporal analyses. *International Journal of Innovative Computing, Information and Control* 8, 6 (2012), 1–11.
- [33] Gaohua Lin, Yongming Zhang, Gao Xu, and Qixing Zhang. 2019. Smoke Detection on Video Sequences Using 3D Convolutional Neural Networks. *Fire Technology* (2019), 1–21.
- [34] Gaohua Lin, Yongming Zhang, Qixing Zhang, Yang Jia, Gao Xu, and Jinjun Wang. 2017. Smoke detection in video sequences based on dynamic texture using volume local binary patterns. *KSH Transactions on Internet and Information Systems* (2017).
- [35] Ji Lin, Chuang Gan, and Song Han. 2019. TSM: Temporal Shift Module for Efficient Video Understanding. In *Proceedings of the IEEE International Conference on Computer Vision*.
- [36] Chris J Lintott, Kevin Schawinski, Anže Slosar, Kate Land, Steven Bamford, Daniel Thomas, M Jordan Raddick, Robert C Nichol, Alex Szalay, Dan Andreescu, et al. 2008. Galaxy Zoo: morphologies derived from visual inspection of galaxies from the Sloan Digital Sky Survey. *Monthly Notices of the Royal Astronomical Society* 389, 3 (2008), 1179–1189.
- [37] Wei Liu, Dragomir Anguelov, Dumitru Erhan, Christian Szegedy, Scott Reed, Cheng-Yu Fu, and Alexander C Berg. 2016. SSD: Single shot multibox detector. In *European conference on computer vision*. Springer, 21–37.
- [38] Yanbei Liu, Wen Qin, Kaihua Liu, Fang Zhang, and Zhitao Xiao. 2019. A Dual Convolution Network Using Dark Channel Prior for Image Smoke Classification. *IEEE Access* 7 (2019), 60697–60706.
- [39] Gwen Ottinger. 2017. Making sense of citizen science: stories as a hermeneutic resource. *Energy research & social science* 31 (2017), 41–49.
- [40] Adam Paszke, Sam Gross, Soumith Chintala, Gregory Chanan, Edward Yang, Zachary DeVito, Zeming Lin, Alban Desmaison, Luca Antiga, and Adam Lerer. 2017. Automatic Differentiation in PyTorch. In *NIPS Autodiff Workshop*.
- [41] C Arden Pope III and Douglas W Dockery. 2006. Health effects of fine particulate air pollution: lines that connect. *Journal of the air & waste management association* 56, 6 (2006), 709–742.
- [42] Vikas C Raykar, Shipeng Yu, Linda H Zhao, Gerardo Hermosillo Valadez, Charles Florin, Luca Bogoni, and Linda Moy. 2010. Learning from crowds. *Journal of Machine Learning Research* 11, Apr (2010), 1297–1322.
- [43] Joseph Redmon and Ali Farhadi. 2017. YOLO9000: better, faster, stronger. In *Proceedings of the IEEE conference on computer vision and pattern recognition*. 7263–7271.
- [44] Shaoqing Ren, Kaiming He, Ross Girshick, and Jian Sun. 2015. Faster r-cnn: Towards real-time object detection with region proposal networks. In *Advances in neural information processing systems*. 91–99.
- [45] Olga Russakovsky, Jia Deng, Hao Su, Jonathan Krause, Sanjeev Satheesh, Sean Ma, Zhiheng Huang, Andrej Karpathy, Aditya Khosla, Michael Bernstein, et al. 2015. Imagenet large scale visual recognition challenge. *International journal of computer vision* 115, 3 (2015), 211–252.
- [46] Henry Sauermann and Chiara Franzoni. 2015. Crowd science user contribution patterns and their implications. *Proceedings of the National Academy of Sciences* 112, 3 (2015), 679–684. <https://doi.org/10.1073/pnas.1408907112> arXiv:<https://www.pnas.org/content/112/3/679.full.pdf>
- [47] Ramprasaath R Selvaraju, Michael Cogswell, Abhishek Das, Ramakrishna Vedantam, Devi Parikh, and Dhruv Batra. 2017. Grad-cam: Visual explanations from deep networks via gradient-based localization. In *Proceedings of the IEEE International Conference on Computer Vision*. 618–626.
- [48] Jennifer Shirk, Heidi Ballard, Candie Wilderman, Tina Phillips, Andrea Wiggins, Rebecca Jordan, Ellen McCallie, Matthew Minarchek, Bruce Lewenstein, Marianne Krasny, et al. 2012. Public participation in scientific research: a framework for deliberate design. *Ecology and society* 17, 2 (2012).
- [49] Karen Simonyan and Andrew Zisserman. 2014. Two-stream convolutional networks for action recognition in videos. In *Advances in neural information processing systems*. 568–576.
- [50] Brian L Sullivan, Christopher L Wood, Marshall J Iliff, Rick E Bonney, Daniel Fink, and Steve Kelling. 2009. eBird: A citizen-based bird observation network in the biological sciences. *Biological Conservation* 142, 10 (2009), 2282–2292.
- [51] Hongta Tian, Wanqing Li, Philip Ogunbona, editor="Cremers Daniel Wang, Lei", Ian Reid, Hideo Saito, and Ming-Hsuan Yang. 2015. *Single Image Smoke Detection*. Springer International Publishing, Chapter Computer Vision – ACCV 2014: 12th Asian Conference on Computer Vision, Singapore, Singapore, November 1-5, 2014, Revised Selected Papers, Part II, 87–101.

- [52] B Uğur Töreyn, Yiğithan Dedeoğlu, and A Enis Cetin. 2005. Wavelet based real-time smoke detection in video. In *2005 13th European Signal Processing Conference*. IEEE, 1–4.
- [53] Computer Vision and Korea Pattern Recognition Laboratory, Keimyung University. n.d.. KMU Fire & Smoke Database. <https://cvpr.kmu.ac.kr/Dataset/Dataset.htm>. (n.d.).
- [54] Xiaolong Wang, Ross Girshick, Abhinav Gupta, and Kaiming He. 2018. Non-local neural networks. In *Proceedings of the IEEE conference on computer vision and pattern recognition*. 7794–7803.
- [55] Gao Xu, Qixing Zhang, Dongcai Liu, Gaohua Lin, Jinjun Wang, and Yongming Zhang. 2019. Adversarial Adaptation From Synthesis to Reality in Fast Detector for Smoke Detection. *IEEE Access* 7 (2019), 29471–29483.
- [56] Gao Xu, Yongming Zhang, Qixing Zhang, Gaohua Lin, and Jinjun Wang. 2017. Deep domain adaptation based video smoke detection using synthetic smoke images. *Fire safety journal* 93 (2017), 53–59.
- [57] Gao Xu, Yongming Zhang, Qixing Zhang, Gaohua Lin, Zhong Wang, Yang Jia, and Jinjun Wang. 2019. Video smoke detection based on deep saliency network. *Fire Safety Journal* 105 (2019), 277–285.
- [58] Zhen Yang, Weilan Shi, Zhiyi Huang, Zhijian Yin, Fan Yang, and Meichen Wang. 2018. Combining Gaussian Mixture Model and HSV Model with Deep Convolution Neural Network for Detecting Smoke in Videos. In *2018 IEEE 18th International Conference on Communication Technology (ICCT)*. IEEE, 1266–1270.
- [59] Zhijian Yin, Boyang Wan, Feiniu Yuan, Xue Xia, and Jinting Shi. 2017. A deep normalization and convolutional neural network for image smoke detection. *Ieee Access* 5 (2017), 18429–18438.
- [60] Feiniu Yuan, Lin Zhang, Boyang Wan, Xue Xia, and Jinting Shi. 2019. Convolutional neural networks based on multi-scale additive merging layers for visual smoke recognition. *Machine Vision and Applications* 30, 2 (2019), 345–358.
- [61] Feiniu Yuan, Lin Zhang, Xue Xia, Boyang Wan, Qinghua Huang, and Xuelong Li. 2019. Deep smoke segmentation. *Neurocomputing* 357 (2019), 248–260.
- [62] Qixing Zhang. n.d.. Research Webpage about Smoke Detection for Fire Alarm: Datasets. <http://smoke.ustc.edu.cn/datasets.htm>. (n.d.).
- [63] Qi-xing Zhang, Gao-hua Lin, Yong-ming Zhang, Gao Xu, and Jin-jun Wang. 2018. Wildland forest fire smoke detection based on faster R-CNN using synthetic smoke images. *Procedia engineering* 211 (2018), 441–446.